

Heat effect of grain boundary wetting in Al-Mg alloys

**O. A. Kogtenkova, S. G. Protasova,
A. A. Mazilkin, B. B. Straumal, P. Zięba,
T. Czeppe & B. Baretzky**

Journal of Materials Science

Full Set - Includes 'Journal of Materials
Science Letters'

ISSN 0022-2461

Volume 47

Number 24

J Mater Sci (2012) 47:8367-8371

DOI 10.1007/s10853-012-6786-3



Your article is protected by copyright and all rights are held exclusively by Springer Science+Business Media, LLC. This e-offprint is for personal use only and shall not be self-archived in electronic repositories. If you wish to self-archive your work, please use the accepted author's version for posting to your own website or your institution's repository. You may further deposit the accepted author's version on a funder's repository at a funder's request, provided it is not made publicly available until 12 months after publication.

Heat effect of grain boundary wetting in Al–Mg alloys

O. A. Kogtenkova · S. G. Protasova ·
A. A. Mazilkin · B. B. Straumal · P. Zięba ·
T. Czeppe · B. Baretzky

Received: 30 April 2012 / Accepted: 2 August 2012 / Published online: 16 August 2012
© Springer Science+Business Media, LLC 2012

Abstract Grain boundary wetting transitions were previously observed in the Al–Mg system. The melting of as-cast Al–5 wt% Mg and Al–10 wt% Mg alloys was studied by the differential scanning calorimetry. The asymmetric shape of the melting curve permitted the observation of the thermal effect of grain boundary wetting. The difference in the shape of the melting curve for the two studied alloys is explained by the different temperature dependence of the fraction of completely wetted grain boundaries.

Introduction

Al–Mg alloys play an important role in the technology of light alloys because of their good combination of strength and ductility [1]. Further improvement of the mechanical properties of Al–Mg alloys is possible by tailoring the grain size, and therefore, the specific area of grain boundaries

(GBs) [2–4]. In the Al–Mg system, the Al GBs can be wetted by the melt or by the second solid phase Al_3Mg_2 [5, 6]. The GB wetting phenomenon is very important in processes such as liquid phase sintering, brazing, welding, or melt infiltration [7–9]. GB wetting has been carefully investigated for many years [10–12]. The GB is completely wetted if the contact angle θ between the GB and melt is zero ($\theta = 0^\circ$). In this case, the GB separating the grains is completely substituted by the liquid phase. The GB is incompletely wetted if the contact angle between the GB and melt is finite, $\theta > 0^\circ$. In this case, the GB can exist in equilibrium contact with the liquid phase. With increasing temperature, the transition proceeds from incomplete to complete GB wetting [5, 6]. The transition from incomplete to complete GB wetting occurs at a certain temperature T_w if the energy of two solid–liquid interfaces $2\sigma_{\text{SL}}$ becomes lower than the GB energy, $\sigma_{\text{GB}} > 2\sigma_{\text{SL}}$. Cahn [13] and Ebner and Saam [14] first showed that the (reversible) transition from incomplete to complete wetting can proceed with increasing temperature, and that it is a true surface transformation. Later, GB wetting transitions were observed in numerous experiments ([5, 6, 15, 16] and references therein). The wetting phase can be liquid [5, 15, 16] as well as solid [6, 17]. Differential scanning calorimetry (DSC) permits us not only to measure the thermal effects of bulk phase transformations but also to characterize the change of GB specific area during grain growth, or the gradual change of amount of completely wetted GBs [18, 19]. DSC investigations of GB wetting transitions in the Al–Mg system is the goal of this work.

Experimental methods

Al–5 wt% Mg and Al–10 wt% Mg alloys were prepared from high-purity components (99.999 % Al and 99.99 %

O. A. Kogtenkova · S. G. Protasova · A. A. Mazilkin ·
B. B. Straumal
Institute of Solid State Physics, Russian Academy of Sciences,
142432 Chernogolovka, Russia

S. G. Protasova · A. A. Mazilkin · B. B. Straumal (✉) ·
B. Baretzky
Karlsruher Institut für Technologie (KIT), Institut für
Nanotechnologie, Hermann-von-Helmholtz-Platz 1,
76344 Eggenstein-Leopoldshafen, Germany
e-mail: straumal@issp.ac.ru; straumal@mf.mpg.de

P. Zięba · T. Czeppe
Institute of Metallurgy and Materials Science, Polish Academy
of Sciences, Reymonta St. 25, 30-059 Cracow, Poland

Mg) by vacuum induction melting and casting into 10-mm diameter rods. The as-cast samples were studied by DSC using TA Instruments calorimeters (models 910 and 1600) in dry nitrogen at cooling and heating rates of 10 K/min. The heating rate of 10 K/min was chosen because at a higher heating rate of 20 K/min, the effects we would like to study became harder to detect. Lower heating rates of 5 or 1 K/min resulted in substantial grain growth, and the loss of GB area. In order to record the DSC curves, the samples were heated from 20 to 670 °C. Transmission electron microscopy (TEM) investigations were carried out using a PHILIPS CM20 microscope at an accelerating voltage of 200 kV.

Results and discussion

Figure 1a presents the microstructure of the as-cast Al–10 wt% Mg alloy. The Al–5 wt% Mg and Al–10 wt% Mg alloys contain grains of (Al) solid solution with a mean size of 50 μm . (The term (Al) here represents the face-centered cubic solid solution phase based on Al). The dislocation density in (Al) is about 10^{12} m^{-2} . The dislocations are distributed non-uniformly and subgrain boundaries are visible. Electron diffraction (Fig. 1b) reveals the presence of the β -phase (Al_3Mg_2). The Al_3Mg_2 particles have a size of about 10 μm . They are probably coherent with the (Al) matrix. The microstructure of the Al–5 wt% Mg alloy is similar to that of the Al–10 wt% Mg alloy. However, the Al–5 wt% Mg alloy contains a lower amount of the β -phase.

In Fig. 2, the temperature dependence of heat flow (DSC curve) is shown for the as-cast Al–5 wt% Mg alloy heated from 20 to 670 °C at a rate of 10 K/min. Only the high-temperature part between 400 and 670 °C is shown in Fig. 2. The integral heat effect of melting (melting enthalpy) was 401.2 J/g. In Fig. 3, a similar DSC curve is shown for the Al–10 wt% Mg alloy. The integral heat of melting was 271.3 J/g. The measured melting heat effect for the Al–5 wt% Mg alloy is close to the melting enthalpy for pure aluminum $399.9 \pm 1.3 \text{ J/g}$ [20], $401.3 \pm 1.6 \text{ J/g}$ [21]. It is known from the literature that the addition of Mg (and Zn) decreases the melting enthalpy effect in Al. For example, it is 329 J/g in the Al–34 wt% Mg–6 wt% Zn alloy [22]. Our observation correlates with this trend.

We used the standard approach for quantification of the DSC curves [23] (these procedures are also included in the quantification software of modern DSC equipment). According to this approach, for melting of an alloy between the solidus and liquidus temperatures, the position of a deep minimum corresponds to the end of melting, i.e., to the liquidus temperature. The measured minimum positions for both samples correspond well to the literature

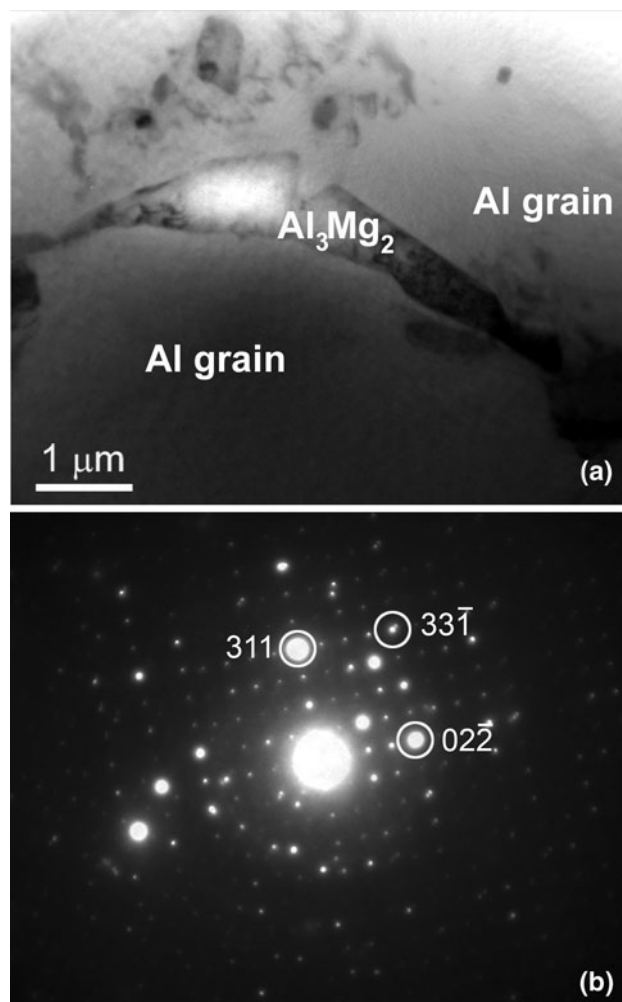


Fig. 1 Bright field TEM micrograph of the Al–10 wt% Mg as-cast alloy (a) and respective electron diffraction pattern (b). The brightest reflections are indicated. They belong to the Al grain. The weak reflections belong to the Al_3Mg_2 grain. Some coherency between Al and Al_3Mg_2 lattices is visible

data for the liquidus temperatures in the Al–Mg system (see Fig. 4, open circles represent the minimum positions) [24]. In the standard case [23], the left side of the DSC minima for melting follows the linear tangent almost until the intersection point with the base line. In our case (Figs. 2, 3), each of the DSC curves deviates from this tangential. The temperatures given by the conventional procedure (i.e., defined using the intersection of the base line and the tangential to the left side of the minimum) are 612.1 °C for the Al–5 wt% Mg alloy (Fig. 2) and 571.7 °C for the Al–10 wt% Mg alloy (Fig. 3). These temperatures lie between the solidus and liquidus temperatures for these alloys (crosses in Fig. 4) [18]. A broad “shoulder” is visible in the left part of each melting minimum (Figs. 2, 3). More importantly, the presence of a secondary, superimposed peak (itself with a minimum) may be interpreted

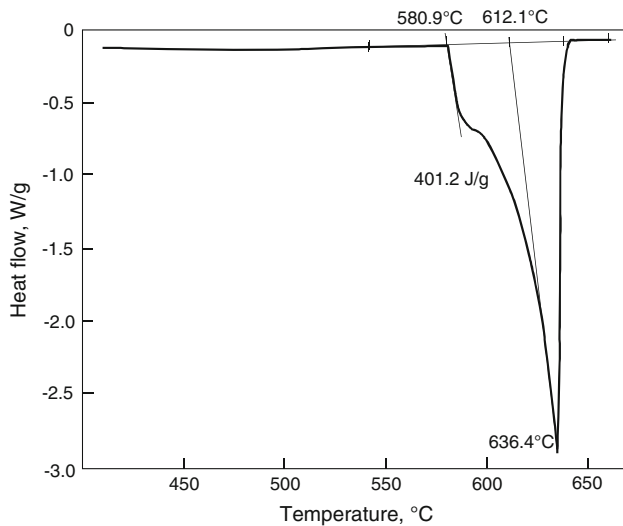


Fig. 2 Temperature dependence of heat flow (DSC curve) for the Al-5 wt% Mg alloy

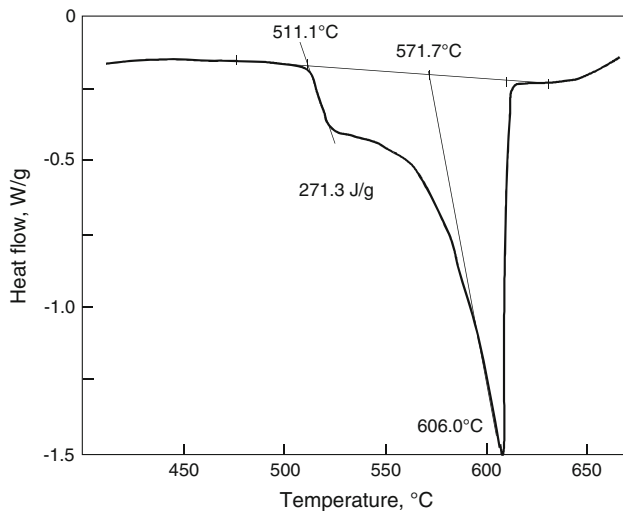


Fig. 3 Temperature dependence of heat flow (DSC curve) for the Al-10 wt% Mg alloy

from Figs. 2 and 3. The “shoulder” is more visible in Fig. 3. These “shoulders” positioned to the left of the main DSC minimum reveal that melting proceeds by two steps. In addition to the “main” melting tangential, it is possible to draw a second tangential at a lower temperature (Figs. 2, 3). The temperatures obtained by the intersection of the second tangential with the base line are 580.9 °C for the Al-5 wt% Mg alloy (Fig. 2) and 511.1 °C for the Al-10 wt% Mg alloy (Fig. 3). They are close to the solidus temperatures of the respective alloys (open squares in Fig. 4) [24]. We suppose that this two-stage melting is driven by the transition from incomplete to complete GB wetting. Such a transition was previously observed in binary Al-Mg and ternary Al-Zn-Mg alloys [5, 25]. During conventional melting, the bulk phase

gradually becomes liquid between the solidus and liquidus lines. In this case, the tangential to the left side of the DSC melting curve intersects the base line almost at the point where the DSC melting curve starts to decline down from the base line. In the case of GB wetting, the portions of the initially melted bulk redistribute along the GBs. This fraction of the melt wets the GBs and separates the remaining solid grains one from another. Due to this process, the melting heat is released at lower temperatures, and the shape of the DSC melting curve changes (Figs. 2, 3). The additional “shoulders” in the DSC curves due to GB wetting and pre-melting effects have been previously observed in Al-Zn alloys [19, 26].

The shape change of the DSC curve depends on the GB character distribution (GBCD). The GBCD determines the GB energy scatter and, therefore, the scatter of GB wetting temperatures, T_w . The main parameter responsible for the spread of wetting temperatures between T_{wmin} and T_{wmax} is the GB anisotropy [27]. Indeed, the anisotropy of the solid-liquid interfacial energy is much lower (within a few % for metallic systems) than that of GBs ([28] and references therein). In principle, the GBCD may also change with temperature [29–31]. The transition from incomplete to the complete GB wetting proceeds if the energy of the two solid-liquid interfaces $2\sigma_{SL}$ becomes lower than the GB energy; $\sigma_{GB} > 2\sigma_{SL}$. The GB wetting temperature T_w , therefore, depends both on the GB energy and the solid-liquid interfacial energy, which in turn depend on the crystallography of these interfaces [32–34]. The transition from incomplete to complete GB wetting starts at a minimum temperature T_{wmin} that corresponds to the combination of maximum σ_{GB} and minimum σ_{SL} . In the Al-Mg alloys, $T_{wmin} = 540$ °C [5]. This is shown by the thin tie-line in the (Al) + L area of the Al-Mg bulk phase diagram (Fig. 4). The transition from incomplete to complete GB wetting finishes at a maximum temperature T_{wmax} that corresponds to the combination of minimum σ_{GB} and maximum σ_{SL} . In the Al-Mg alloys, $T_{wmax} = 610$ °C [5]. This is shown by the second tie-line in the (Al) + L area of the Al-Mg bulk phase diagram (Fig. 4). In the Al-5 wt% Mg alloy, the solidus temperature is about 40 °C higher than $T_{wmin} = 540$ °C (Fig. 4). This means that when the Al-5 wt% Mg alloy starts to melt, many GBs should become completely wetted at once. The heat of this GB wetting process is localized in the narrow temperature interval slightly above the solidus temperature. As a result, the cross marking the position of first tangential appears almost in the middle between the solidus and liquidus temperatures (Fig. 2). In the Al-10 wt% Mg alloy, the solidus temperature is lower than T_{wmin} , and the liquidus temperature is close to $T_{wmax} = 610$ °C (Fig. 4). This means that all GBs become completely wetted between the solidus and liquidus temperatures one after another. As a

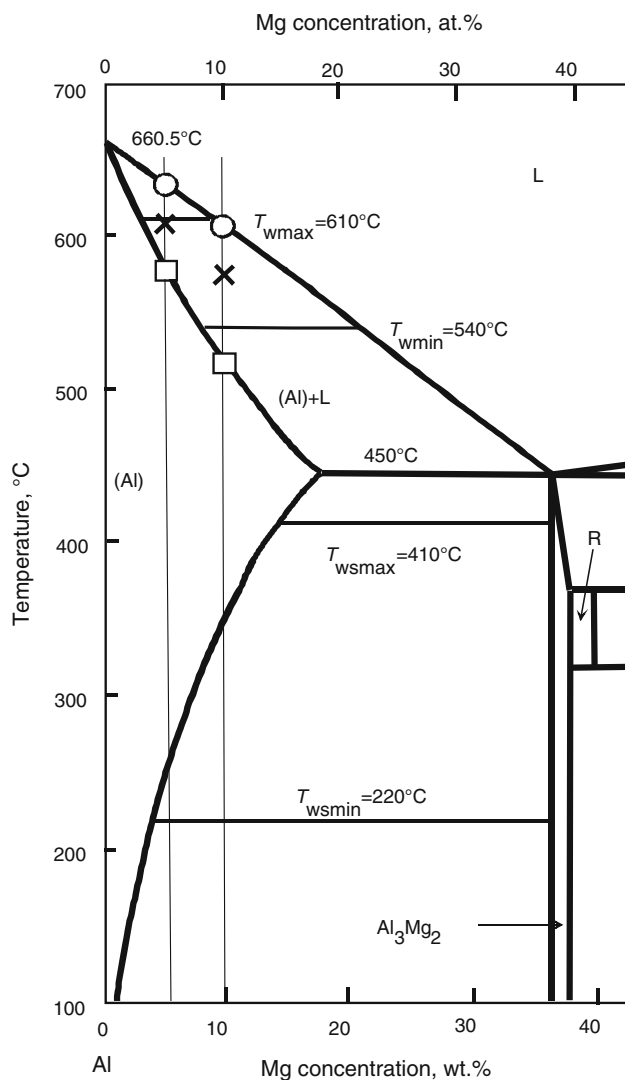


Fig. 4 Part of the Al–Mg phase diagram, reproduced with permission from Straumal et al. [19]. *Thick lines* denote the bulk phase transitions [24]. *Thin horizontal lines* are the tie-lines of GB wetting phase transitions. T_{wmax} and T_{wmin} for GB wetting by the liquid phase are taken from Ref. [5]. T_{wsmax} and T_{wsmin} for GB wetting by a second solid phase Al_3Mg_2 were determined in Ref. [19]. *Vertical thin lines* mark the composition of the studied alloys. *Circles* denote the positions of the minima in the DSC curves (Figs. 2, 3). *Crosses* mark the positions of intersection of the first tangential with the DSC base line. *Squares* denote the positions of intersection of the second tangential with the DSC base line

result, the “shoulder” in the melting curve for the Al–10 wt% Mg alloy is broader (Fig. 3). The intersection of the first tangential with the base line is closer to the liquidus temperature (Figs. 3, 4). A similar tendency can be observed in the ternary Al–Zn–Mg alloys. The solidus temperature in the Al–5 wt% Zn–2 wt% Mg alloy is about 550 °C [25]. This is very close to $T_{wmax} = 585$ °C [25]. As a result, many (Al) GBs become wetted immediately above the solidus temperature. The intersection of the first tangential with the DSC base line is almost in the middle

between the solidus and liquidus temperatures [19]. The solidus temperature in the Al–10 wt% Zn–4 wt% Mg alloy is about 500 °C [25]. In this alloy, the GB wetting temperatures T_w are more uniformly distributed between the solidus and liquidus temperatures. The intersection of the first tangential with the DSC base line is shifted toward the liquidus [19].

Summary and conclusions

The transition from incomplete to complete GB wetting in binary Al–Mg alloys causes an asymmetric shape of the melting curve measured by DSC. The shape of the “shoulder” in the melting curve depends on the position of GB wetting tie-lines between the solidus and liquidus temperatures. Thus, when the Al–5 wt% Mg alloy starts to melt, many GBs should become completely wetted at once. The heat of this GB wetting process is localized in the narrow temperature interval slightly above the solidus temperature. For the Al–10 wt% Mg alloy, the solidus temperature is lower than the minimum temperature of the wetting transition T_{wmin} , and the liquidus temperature is close to the maximum temperature of the wetting transition $T_{wmax} = 610$ °C. This means that all GBs become completely wetted between the solidus and liquidus temperatures, one after another. As a result, the “shoulder” in the melting curve for the Al–10 wt% Mg alloy is broader than that for the Al–5 wt% Mg alloy. The observed effect deserves more detailed investigation. In particular, the evolution of the GBCD during a DSC experiment has to be studied using EBSD, as well as the influence of GBCD on the thermal effect of GB wetting.

Acknowledgements Authors thank the Russian Foundation for Basic Research (contract 11-03-01198), Program of bilateral cooperation between Russian and Polish Academies of sciences, the grant of President of Russian Federation for young scientists (MK-3748.2011.8), and Polish National Science Centre (grant UMO-2011/01/M/ST8/07822) for the financial support. Authors cordially thank Prof. R.Z. Valiev and Dr. A. Gornakova for stimulating discussions.

References

1. Furukawa M, Horita Z, Nemoto M, Valiev RZ, Langdon TG (1996) *Acta Mater* 44:4619
2. Mazilkin AA, Straumal BB, Rabkin E, Baretzky B, Enders S, Protasova SG, Kogtenkova OA, Valiev RZ (2006) *Acta Mater* 54:3933
3. Roven HJ, Liu M, Murashkin MY, Valiev RZ, Kilmametov AR, Ungár T, Balogh L (2008) *Mater Sci Forum* 604:179
4. Lee Z, Zhou F, Valiev RZ, Lavernia EJ, Nutt SR (2004) *Scripta Mater* 51:209
5. Straumal BB, López G, Mittemeijer EJ, Gust W, Zhilyaev AP (2003) *Def Diff Forum* 216:307
6. Straumal BB, Baretzky B, Kogtenkova OA, Straumal AB, Sidorenko AS (2010) *J Mater Sci* 45:2057. doi:10.1007/s10853-009-4014-6

7. German RM, Suri P, Park SJ (2009) *J Mater Sci* 44:1
8. Watson EB (1982) *Geology* 10:236
9. Laporte D, Watson EB (1995) *Chem Geol* 124:161
10. Gabrisch H, Dahmen U, Johnson E (1998) *Microsc Res Tech* 42:241
11. Felberbaum L, Rossoll A, Mortensen A (2005) *J Mater Sci* 40:3121. doi:[10.1007/s10853-005-2673-5](https://doi.org/10.1007/s10853-005-2673-5)
12. Empl D, Felberbaum L, Laporte V, Chatain D, Mortensen A (2009) *Acta Mater* 57:2527
13. Cahn JW (1977) *J Chem Phys* 66:3667
14. Ebner C, Saam WF (1977) *Phys Rev Lett* 38:1486
15. Straumal BB, Gust W (1996) *Mater Sci Forum* 207:59
16. Straumal BB, Gust W, Watanabe T (1999) *Mater Sci Forum* 294:411
17. López GA, Mittemeijer EJ, Straumal BB (2004) *Acta Mater* 52:4537
18. Amouyal Y, Divinski SV, Klinger L, Rabkin E (2008) *Acta Mater* 56:5500
19. Straumal BB, Kogtenkova OA, Protasova SG, Zięba P, Czeppe T, Baretzky B, Valiev RZ (2011) *J Mater Sci* 46:4243. doi:[10.1007/s10853-011-5257-6](https://doi.org/10.1007/s10853-011-5257-6)
20. Stølen S, Grønvold F (1999) *Thermochim Acta* 327:1
21. Della Gatta G, Richardson M, Sarge SM et al. (2006) *Pure Appl Chem* 78:1455
22. Sun JQ, Zhang RY, Liu ZP et al (2007) *Energy Convers Manag* 48:619
23. Dean JA (1995) *The analytical chemistry handbook*. McGraw Hill, New York (Standards ASTM D 3417, ASTM D 3418, ASTM E 1356, ISO 11357)
24. Massalski TB (ed) (1990) *Binary alloy phase diagrams*. ASM International, Materials Park
25. Straumal BB, Kogtenkova O, Zięba P (2008) *Acta Mater* 56:925
26. Straumal B, Valiev R, Kogtenkova O, Zieba P, Czeppe T, Bielanska E, Faryna M (2008) *Acta Mater* 56:6123
27. Wynblatt P, Takashima M (2001) *Interface Sci* 9:265
28. Chatain D (2008) *Ann Rev Mater Res* 38:45
29. Randle V, Rohrer GS, Hu Y (2008) *Scr Mater* 58:183
30. Downey ST II, Bembridge N, Kalu PN, Miller HM, Rohrer GS, Han K (2007) *J Mater Sci* 42:9543. doi:[10.1007/s10853-007-1959-1](https://doi.org/10.1007/s10853-007-1959-1)
31. Bernardini J, Chatain D, Monchoux JP, Rabkin E (2002) *J Physique IV* 12:229
32. Straumal BB, Polyakov SA, Mittemeijer EJ (2006) *Acta Mater* 54:167. doi:[10.1016/j.actamat.2005.08.037](https://doi.org/10.1016/j.actamat.2005.08.037)
33. Schöllhammer J, Baretzky B, Gust W, Mittemeijer E, Straumal B (2001) *Interface Sci* 9:43. doi:[10.1023/A:1011266729152](https://doi.org/10.1023/A:1011266729152)
34. Straumal BB, Klinger LM, Shvindlerman LS (1984) *Acta Metall* 32:1355. doi:[10.1016/0001-6160\(84\)90081-6](https://doi.org/10.1016/0001-6160(84)90081-6)